

LA-UR-01-4098

Approved for public release;
distribution is unlimited.

Title:

High-energy characterization of two large-volume multi-element CdZnTe detectors

Author(s):

**Calvin E. Moss, Michael C. Browne,
Kiril D. Ianakiev and Thomas H. Prettyman**

Submitted to:

<http://lib-www.lanl.gov/cgi-bin/getfile?00796668.pdf>

Los Alamos National Laboratory, an affirmative action/equal opportunity employer, is operated by the University of California for the U.S. Department of Energy under contract W-7405-ENG-36. By acceptance of this article, the publisher recognizes that the U.S. Government retains a nonexclusive, royalty-free license to publish or reproduce the published form of this contribution, or to allow others to do so, for U.S. Government purposes. Los Alamos National Laboratory requests that the publisher identify this article as work performed under the auspices of the U.S. Department of Energy. Los Alamos National Laboratory strongly supports academic freedom and a researcher's right to publish; as an institution, however, the Laboratory does not endorse the viewpoint of a publication or guarantee its technical correctness.

High-energy characterization of two large-volume multi-element CdZnTe detectors

Calvin E. Moss^{*}, Michael C. Browne, Kiril D. Ianakiev, Thomas H. Prettyman
Los Alamos National Laboratory

ABSTRACT

We present results of experiments to characterize two large-volume, multi-element CdZnTe detectors for gamma-ray spectroscopy at high energy. The first detector consisted of four 1.5 cm × 1.5 cm × 0.75 cm coplanar grid detectors. The measurements for the four-element design were performed with various configurations. The second detector consisted of eight 1 cm × 1 cm × 0.5 cm coplanar grid detectors arranged in a 2 × 2 × 2 array. The high-energy gamma-ray sources included ⁶⁰Co(1332), ²²⁸Th(2614), ²⁴⁴Cm/¹³C(6129), and Fe(n,γ)(7645). The front-end electronics consisted of eight spectroscopy-grade preamplifiers/shapers/pulse stretchers, built on circuit boards close to the arrays. For the four-element measurements the shapers/pulse stretchers were replaced with commercial amplifiers. An eight-channel data acquisition system with list mode output was used to record gamma-ray events for each detector element in each array. The list mode data were analyzed to produce coincidence and singles spectra and efficiencies for the various sources. The Compton continuum and the escape peaks are suppressed in the coincidence spectra relative to the singles spectra. We compare these spectra and efficiencies at high energy to results at lower energies and to Monte Carlo predictions.

Keywords: CdZnTe, gamma-ray detector, array, planetary science, semiconductor, coplanar grid, room temperature

1. INTRODUCTION

Knowledge of the elemental composition of a planetary body is required to understand the formation and evolution of that body. One technique for determining the composition is based on measuring the gamma-ray emission lines produced by cosmic ray bombardment of the surface and by natural radioactivity. The cosmic rays, typically protons with energies up to 10 GeV, cause spallation reactions that produce neutrons in a planetary surface. The neutrons cause (n,n'γ) and (n,γ) reactions yielding characteristic gamma rays with energies up to 10 MeV that can be used to identify the target elements. The elements of most interest for studying planetary bodies are H, O, Si, Al, Mg, Fe, Ti, and Ca. More details of the expected emission lines are provided in an earlier report.¹

Measurements of the cosmic-ray produced emission lines can be performed from orbit or on landers or rovers. The most likely application is from orbit, as was done during the Apollo program² and the Lunar Prospector.³ This technique can provide a global map of the elemental composition. With a lander or rover other in situ techniques are possible, such as active interrogation with a manmade radioactive source or a neutron generator. Sample return missions are being planned to Mars and possibly other bodies. However, these other types of missions do not obviate the need for global mapping missions.

Orbital missions require detectors with good resolution and high efficiency. Scintillator detectors, such as NaI(Tl), CsI(Tl), and BGO, provide high efficiency and but low resolution. Germanium detectors provide excellent resolution but require cooling to about 100 K. CdZnTe detectors have been manufactured with good resolution and peak shape using substrates 15 × 15 × 15 mm³. This volume is not sufficient for gamma rays up to 10 MeV. To achieve adequate volume we proposed a 3 × 3 × 3 array of 15 × 15 × 15 mm³ detector elements in our earlier reports.^{1,4} The signals from the individual detectors would be combined to achieve an efficiency much larger than the efficiency of any one element. However, the manufacturers' yield of spectroscopy grade 15 × 15 × 15 mm³ detectors is low and the costs are high. The largest single crystals readily available at present are on the order of 15 × 15 × 7.5 mm³.

^{*} cmoss@lanl.gov; phone 1 505 667-5066; fax 1 505 665-3657; <http://www.lanl.gov>; Los Alamos National Laboratory, MS J562, Los Alamos, NM 87545

We have acquired four such $15 \times 15 \times 7.5 \text{ mm}^3$ detectors and constructed a multi-channel digital signal processing system. In an earlier report⁴ we described the results obtained from two of these detectors with analog electronics. In the present report we describe the results obtained by operating all four detector elements simultaneously with the digital electronics. In another earlier report⁵ we described the low-energy results from operating eight $10 \times 10 \times 5 \text{ mm}^3$ detector elements simultaneously. In the present report we describe the response of the eight-element array to higher energy gamma rays.

2. EXPERIMENTAL DETAILS

2.1 Detectors

Table 1 lists the parameters provided by the manufacturer for the detectors used in the four-element array. We verified the resolutions at 662 keV before installing the detector elements in the array.

Table 1. Parameters for the $15 \times 15 \times 7.5 \text{ mm}^3$ detectors

Serial Number	Bias (V)	Grid Bias (V)	Resolution FWHM (keV) @ 662 keV	Resolution FWHM (keV) @ 122 keV
I9-02	-1500	-50	21.4	8.2
I9-09	-1400	-50	17.5	7.5
I9-15	-1400	-50	26	10
I9-17	-1500	-50	24.0	9.5

The two configurations and the source positions used for the four-element array measurements are shown in Figure 1. The cathodes were oriented up in these configurations. The detectors were encapsulated in thin polyimide boxes to provide protection and facilitate handling.⁴ The planar configuration provides the maximum area and gives the largest efficiency at low energies. The corner configuration (Figure 1b) is supposed to represent one corner of our proposed $3 \times 3 \times 3$ array. The radioactive sources were placed at the top and side positions shown in order to acquire spectra. In addition, a few spectra were acquired with the sources 2 cm above the planar configuration and 1 cm above the corner configuration in order to obtain better counting rates.

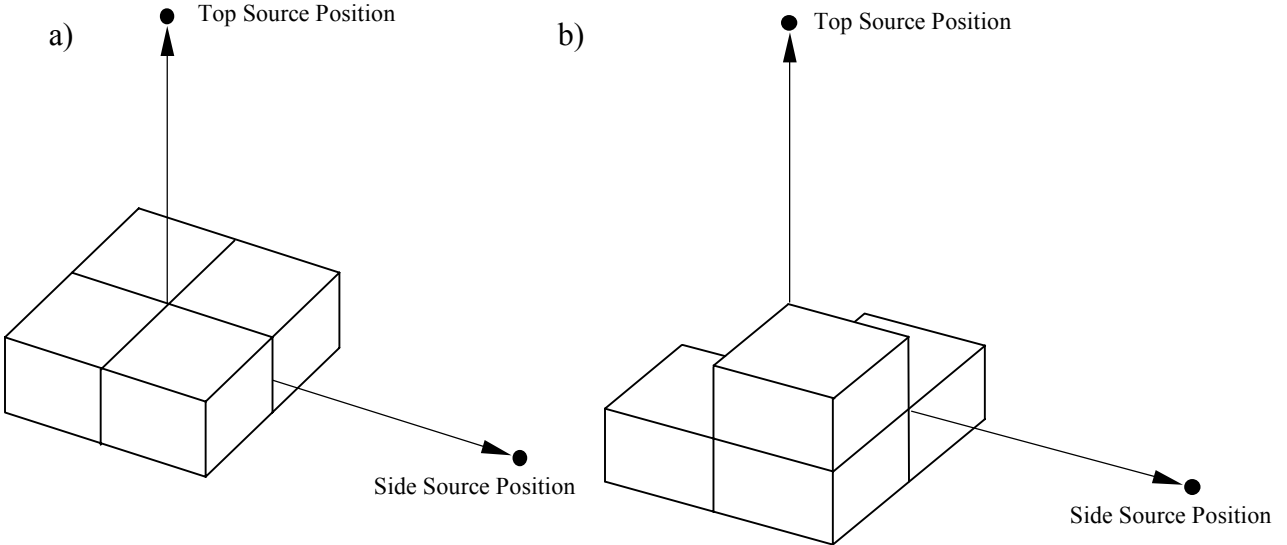


Figure 1: a) Planar configuration and b) corner configuration used for four-element detector measurements.

The eight-element detector has been described previously.⁵ It consists of two planes, each containing four $10 \times 10 \times 5 \text{ mm}^3$ coplanar-grid detector elements. Figure 2a shows a picture of the top plane of detectors; Figure 2b shows the front-end electronics surrounding the eight-element detector.

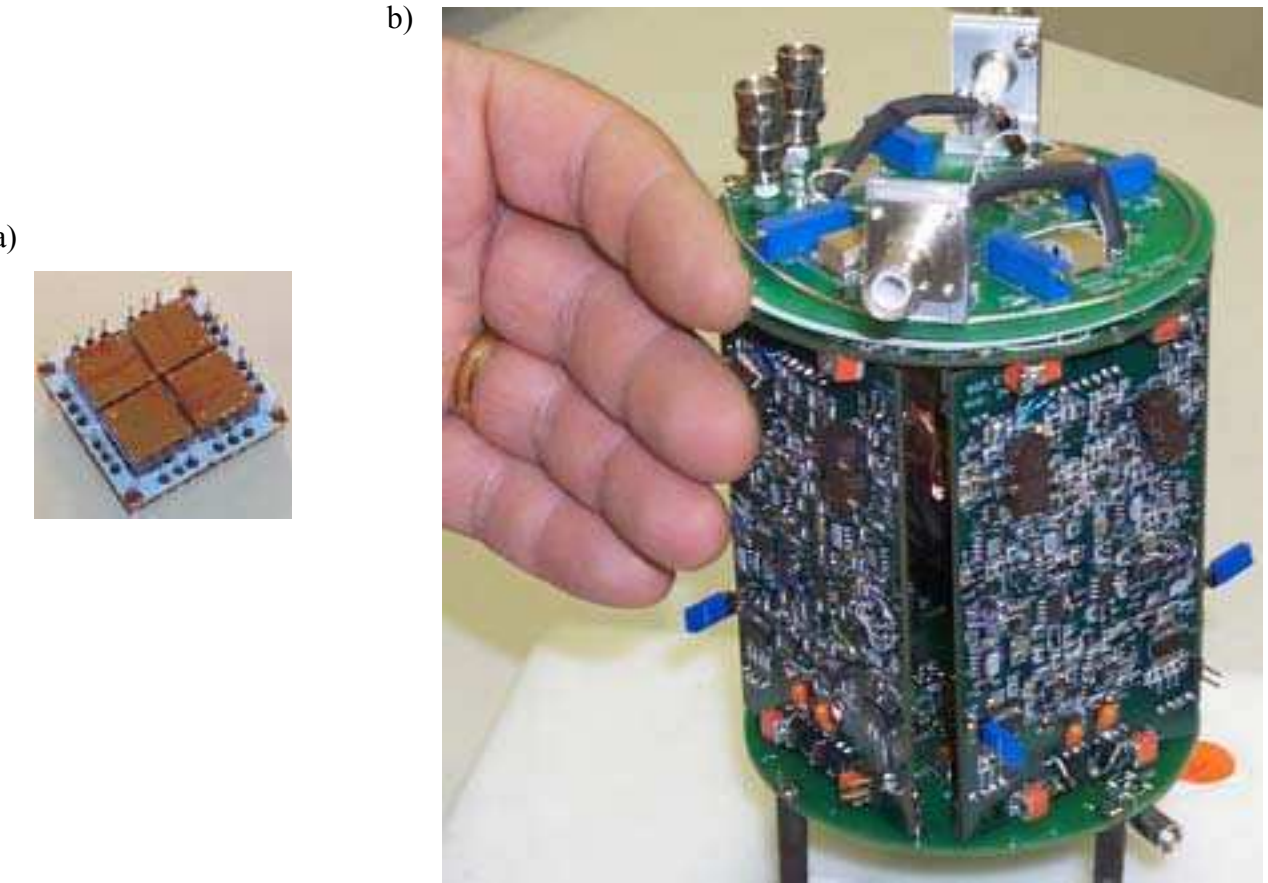


Figure 2. Eight-element detector. a) Top 2×2 array of detector elements mounted on a ceramic substrate. b) Front-end electronics surrounding the $2 \times 2 \times 2$ array.

2.2 Radioactive sources

The following sources, each with a nominal strength of $10 \mu\text{Ci}$ were placed, one at a time, at the positions shown in Figure 1: $^{137}\text{Cs}(662)$, $^{54}\text{Mn}(835)$, $^{88}\text{Y}(898,1836)$, $^{60}\text{Co}(1173,1332)$, and $^{22}\text{Na}(1275)$. The active source material in each source was less than 3 mm in diameter. The strength of each source when it was used was calculated from the certificate provided by the manufacturer. A ^{228}Th source that was encapsulated in small cylinder 7 mm (dia) \times 5 mm (length) provided a 2614-keV line from the daughter ^{208}Tl . A 6129-keV line was provided by the reaction $^{13}\text{C}(\alpha,\text{n}\gamma)^{16}\text{O}$ in a $^{244}\text{Cm}/^{13}\text{C}$ source contained in a small lead cylindrical shield 34 mm (dia) \times 70 mm (length). In use the shield was oriented so that the gamma rays were emitted through the bottom end of the cylindrical shield. The strengths of the ^{228}Th and the $^{244}\text{Cm}/^{13}\text{C}$ sources were measured with a germanium detector that had been absolutely calibrated with various sources and the $^{27}\text{Al}(\text{p},\gamma)^{28}\text{Si}$ reaction.

The measurements were extended to higher energy with the reaction $\text{Fe}(\text{n},\gamma)$. A ^{252}Cf source emitting 10^7 neutrons/second was placed in a well in a massive steel shield, 38 cm \times 38 cm \times 38 cm, and the array was placed approximately 10 cm from one side of shield. This provided a 7631,7645-keV doublet, which was not resolved by the CdZnTe detector array. No attempt was made to determine the absolute strength of the gamma-ray emissions for this extended source.

2.3 Electronics

The circuit used for the four-element array is shown in Figure 3. The circuit boards are different from the boards for the eight-element array because the boards had to be larger in area to accommodate the larger detector elements. The larger boards allowed a different design of the circuit. As with the eight-element array (Figure 2b), the boards with their surface mount components surround the detector (Figure 4). Each detector element is connected to two preamplifiers and a difference circuit, which is the standard configuration for coplanar grid detectors. For the four-element detector the output

from each difference circuit was fed to a commercial spectroscopy-grade shaping amplifier. A signal derived from the base line restorer (BLR) in each amplifier was used as a trigger to the eight-channel ADC.

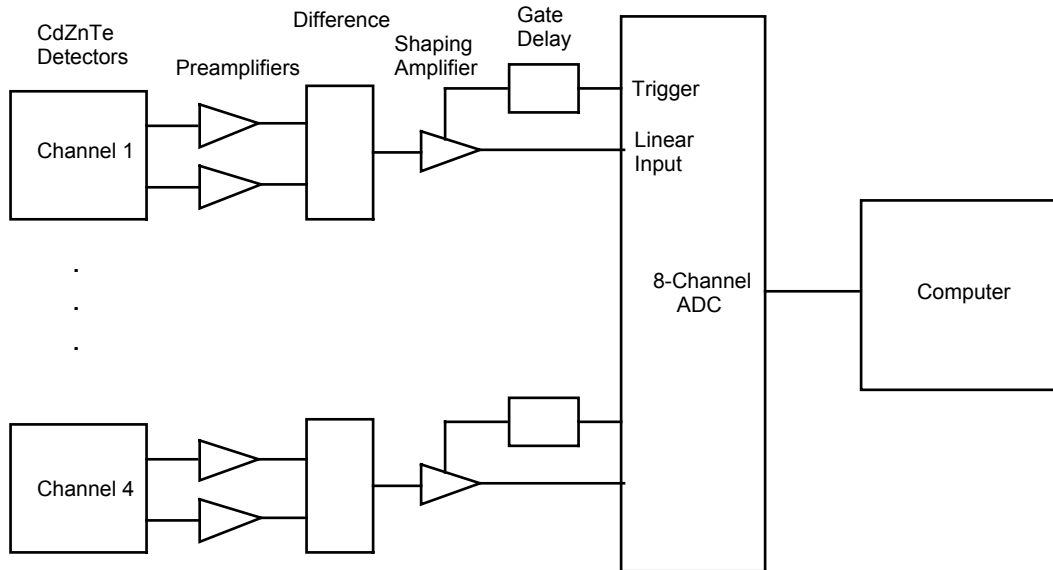


Figure 3. Block diagram of the electronics used for the four-element detector measurements.

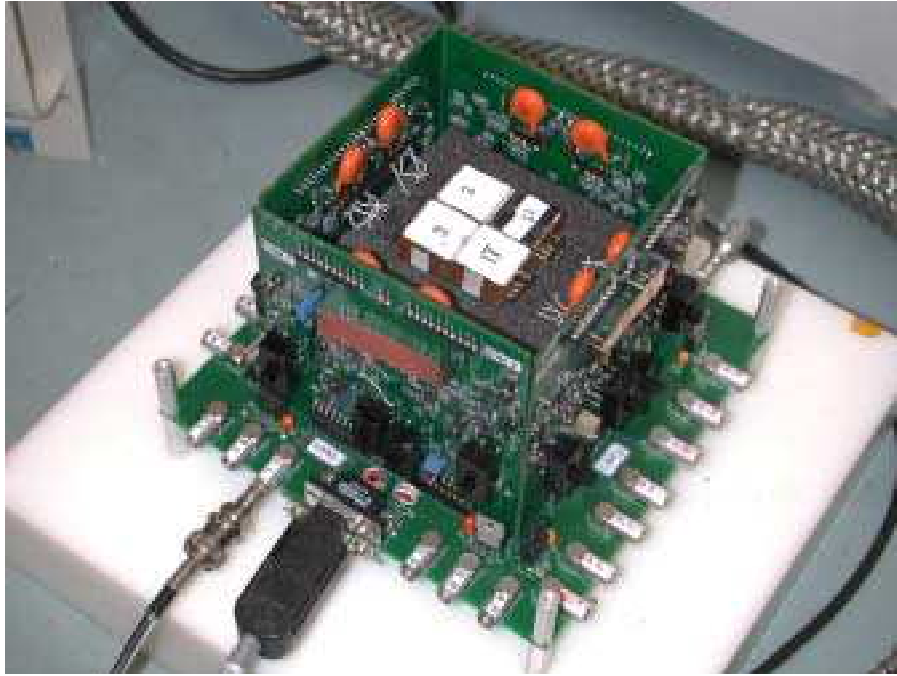


Figure 4. Four-element detector. The top electronics board has been removed.

The electronics used for the eight-element detector were very similar and has been described previously.⁵ The main difference was that electronics pulse shaping amplifiers (CR-RC⁴ with gated BLR and adaptive noise threshold) that were included on the circuit boards in place of the commercial amplifiers.

The data acquisition system was based on the DAQ system developed at the University of Washington for the Sudbury Neutrino Observatory.⁶ The system is based on an eight-channel 6U VME ADC card that is programmed and controlled via a fiber optic link to the computer. Only one card was required for our measurements, but more cards could be used for larger arrays. Each channel of the ADC is equipped with a 32-bit clock module with 250-ns resolution (reprogrammable to 50 ns) for time tagging events. Data were acquired independently in each channel. The data were stored in list mode and for each event consisted of the pulse amplitude as measured by the ADC, the channel number, and the time of the event. This approach generated large data files but allowed complete flexibility in off-line analysis.

2.4 Software

The analysis code was written with Igor ProTM, a commercially available analysis/acquisition package. A linear energy calibration was calculated for each channel from a subset of the gamma-ray lines (in keV) at 122 (⁵⁷Co), 662 (¹³⁷Cs), 835 (⁵⁴Mn), 1173 (⁶⁰Co), and 1332 (⁶⁰Co). A spectrum for each channel could be determined by simply sorting the list-mode data by channel number. For coincidence events, that is, events with interaction in more than one detector element, the energies from the participating channels were normalized before summing the outputs of the channels into a combined spectrum. We determined which events were in coincidence by sorting on time with a 2 μ s window. This window was determined from a time-between-event histogram. The coincidence events were categorized by the number of detector elements participating: 2, 3, 4, or 5. The program also determined peak areas and widths (FWHM) after subtracting a linear background for the full energy, first escape, and second escape peaks.

3. RESULTS

3.1 Four-element detector

Figure 5 shows results for the array of four detector elements in the corner configuration and the source at the top position (Figure 1b). The spectra show the response to the following energies (keV): ¹³⁷Cs, 662; ⁶⁰Co, 1332; ²²⁸Th, 2614; ²⁴⁴Cm/¹³C, 6129; and Fe(n,γ), 7631, 7645. The spectra labeled “Singles” are the sum of all events in which the incident gamma ray only interacted with one detector element. The spectra labeled “Channel 4” are all events in which the incident gamma ray only interacted with the channel 4 detector element. The spectra labeled “coincidence” are the sum of all events in which the incident gamma ray interacted with two or more detector elements. The Compton continuum is greatly reduced in the coincidence spectra. However, the coincidence full energy peak is reduced relative to the singles full energy peak. The Compton continuum is greatly reduced in the coincidence spectra. The counting rate in channel 4, which corresponds to the top detector in Figure 1b, is approximately one fourth of the counting rate of the counting rate in the singles spectrum, which is the sum of four detector elements. At 6129 keV the full energy, single escape, and double escape peaks are clearly visible in the four-element detector (Figure 5d). At 7631-7645 keV only the double escape is clearly visible. The strong line at 2223 keV is produced by neutron capture on hydrogen in the concrete and other material in the room. Spectra from all of the sources taken with the corner configuration and the source at the side position (Figure 1b) as well as spectra taken with the planar configuration and the source at the top and side positions (Figure 1a) are very similar.

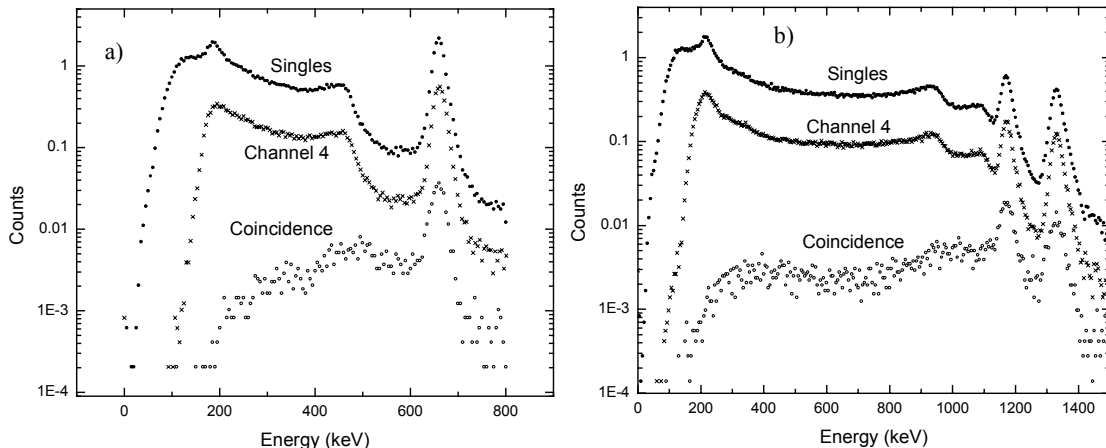


Figure 5. Spectra from the array of four $15 \times 15 \times 7.5 \text{ mm}^3$ detector elements. a) ¹³⁷Cs, b) ⁶⁰Co, c) ²²⁸Th, d) ²⁴⁴Cm/¹³C, and e) Fe(n,γ). The full energy (fe), single escape (se), and double escape (de) peaks are labeled.

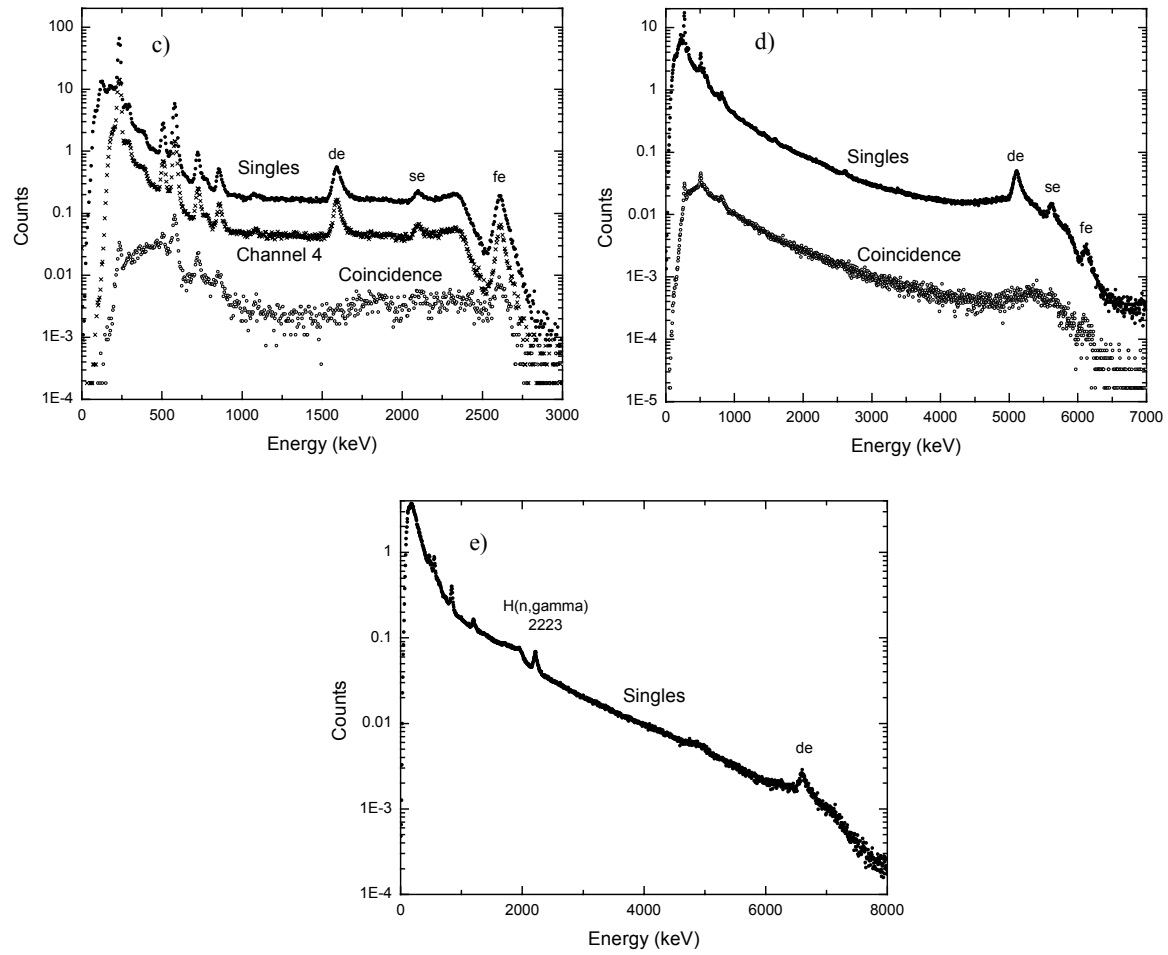


Figure 5 (continued)

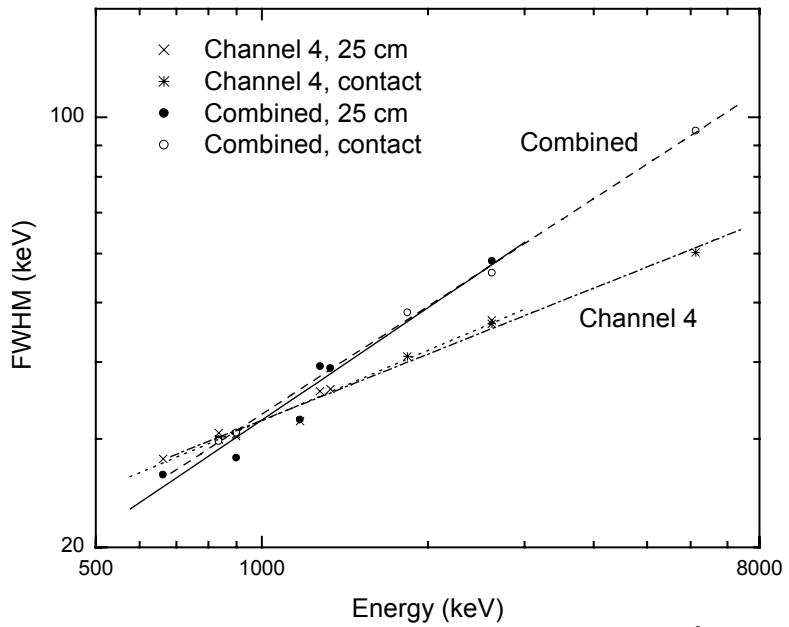


Figure 6. Resolution FWHM in keV for the array of four $15 \times 15 \times 7.5 \text{ mm}^3$ detector elements.

Figure 6 shows the resolution as a function of energy for the array of four detector elements. The configuration for these measurements is shown in Figure 1a. Four sets of data are shown. The set labeled “Combined, 25 cm” was taken with the sources at the top position in Figure 1a. The set labeled “Combined, contact” was taken with the sources in contact with the top electronics board and at a distance of 2 cm from the array surface in order to obtain good counting rates at the higher energies. Similarly, the sets labeled “Channel 4, 25 cm” and “Channel 4, contact” are taken from just the channel four detector element at the two positions 25 cm and contact, respectively. For the “Combined” results the singles and coincidence spectra (Figure 5) were combined. The lines are linear fits on a log-log plot. For channel 4 the fit to the contact resolution is 26.4 keV (4.4%) at 600 keV and 67.6 keV (0.8%) at 8000 keV. For the combined spectra the fit to the contact resolution is 24.6 keV (4.1%) at 600 keV and 110.5 keV (1.4%) at 8000 keV. The resolutions in the channel 4 spectra are better than the resolutions of the singles spectra or the coincidence spectra, except at low energy, which is not statistically significant. Note that a detector element is only included in a sum when the signal from that element exceeds a thresholds so that the increase in noise with an increase in the number of detector elements is minimized. The measured resolutions at the other positions in Figure 1 are similar.

Figures 7a and 7b show the absolute efficiency in the planar (Figure 1a) and corner (Figure 1b) configurations, respectively. The lines are linear fits on a log-log plot. The efficiency for channel four is approximately one fourth of the efficiency for the all four detector elements, as expected. The efficiencies at the other 25-cm positions in Figure 1 are similar to efficiencies at these positions. At high energies the double escape efficiency is larger than the full energy efficiency (Figures 5c, 5d and 5e).

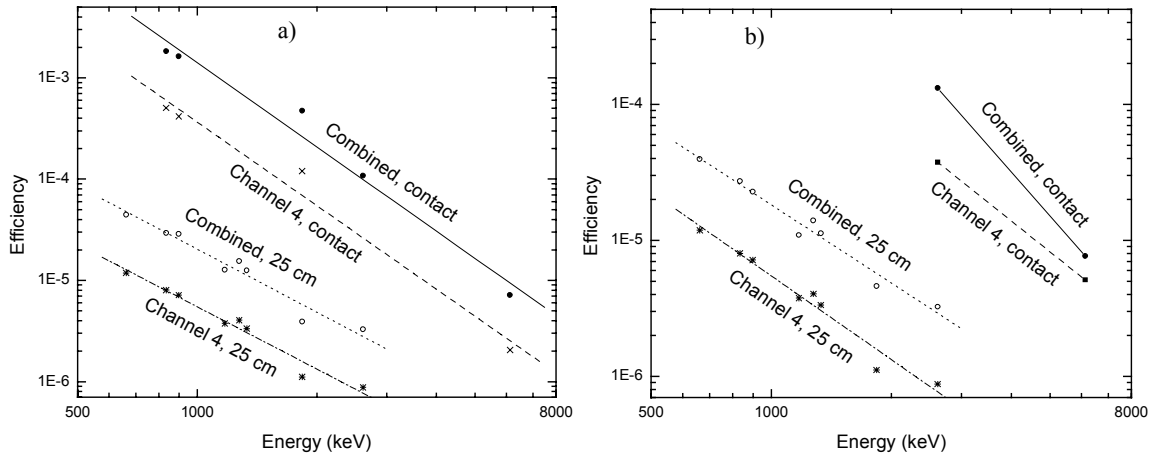


Figure 7. Absolute efficiency of the array of four $15 \times 15 \times 7.5 \text{ mm}^3$ detector elements. a) Planar configuration. b) Corner configuration.

3.2 Eight-element detector

Figure 8 shows results for the array of eight detector elements. The spectra show the response to a range of energies (keV): ^{137}Cs , 662; ^{60}Co , 1332; ^{228}Th , 2614; and $^{244}\text{Cm}/^{13}\text{C}$, 6129. These are the same energies used for the four-element detector except that the highest energy, 7645, is missing. The fact that these detector elements, $10 \times 10 \times 5 \text{ mm}^3$, are smaller than the detector elements, $15 \times 15 \times 7.5 \text{ mm}^3$, in the four-element detector results in less enhancement of the full-energy peaks relative to the continuum and a decrease in the counting rate. The counting rate in the channel 7 spectra is approximately one eighth of the counting rate in the singles spectra, which is the sum of eight detector elements. The area of the double escape exceeds the area of the full energy peak at 2614 keV, but the double escape is suppressed in the coincidence spectrum (Figure 8a). At 6129 keV the double escape peak is even more dominant and the full energy peak is extremely weak with these small detector elements.

Figure 9 shows the resolution as a function of energy for the array of eight detector elements. The lines are linear fits on a log-log plot. For channel 7 the fit resolution is 16.8 keV (2.8%) at 600 keV and 75.7 keV (2.5%) at 3000 keV. For the combined spectra the fit resolution is 21.9 keV (3.7%) at 600 keV and 86.1 keV (2.9%) at 3000 keV. The resolution percentage is expected to be smaller at higher energies.

Figure 10 shows the absolute efficiency as a function of energy for the array of eight detector elements. The efficiency was measured with the source at a distance of 19.8 cm from closest surface of the array.⁵ The lines are linear fits on a log-log plot.

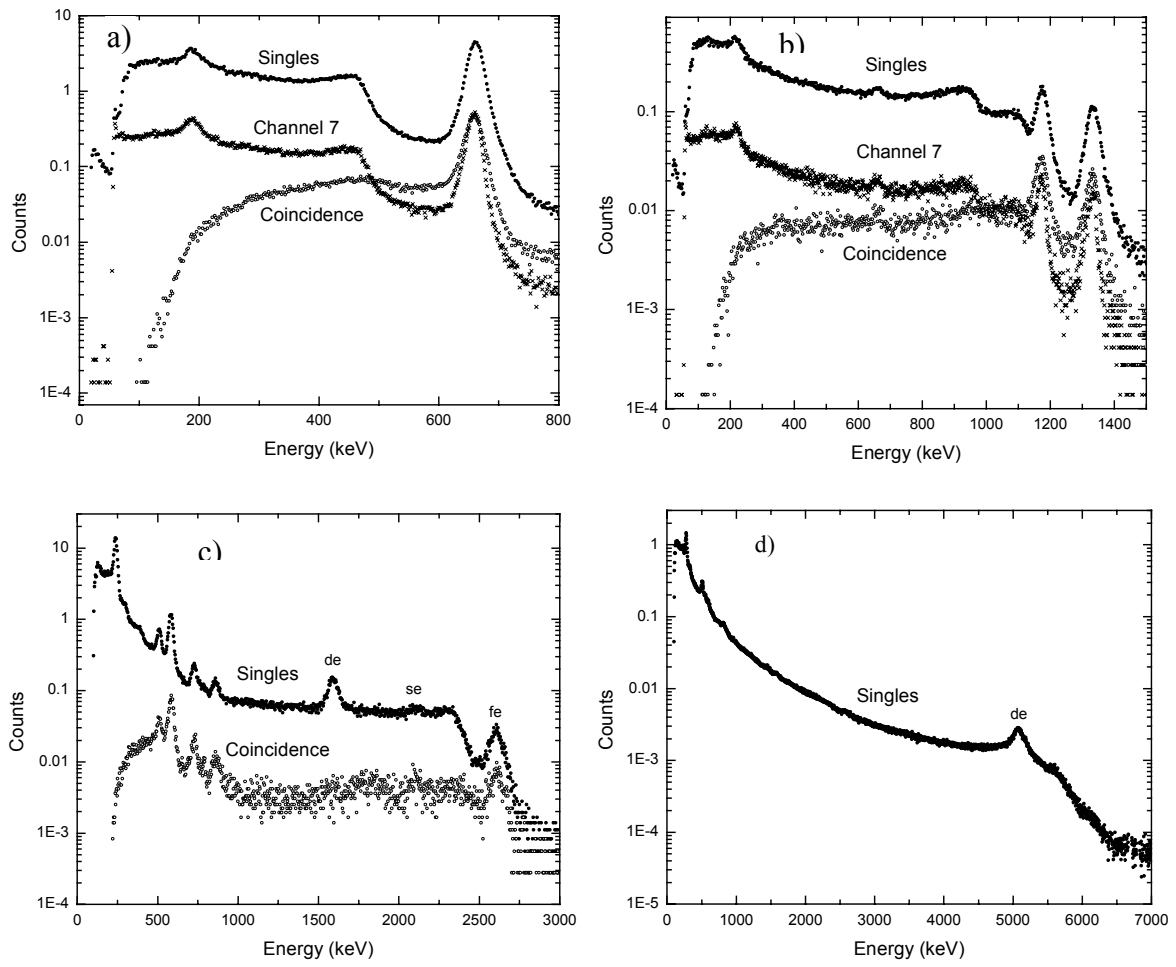


Figure 8. Spectra from array of eight $10 \times 10 \times 5 \text{ mm}^3$ detector elements. a) ^{137}Cs , b) ^{60}Co , c) ^{228}Th , and d) $^{244}\text{Cm}/^{13}\text{C}$

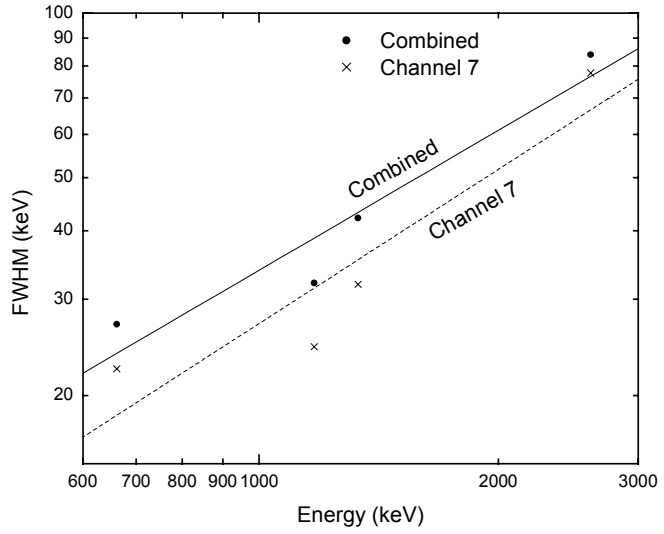


Figure 9. Resolution FWHM in keV for the array of eight $10 \times 10 \times 5 \text{ mm}^3$ detector elements.

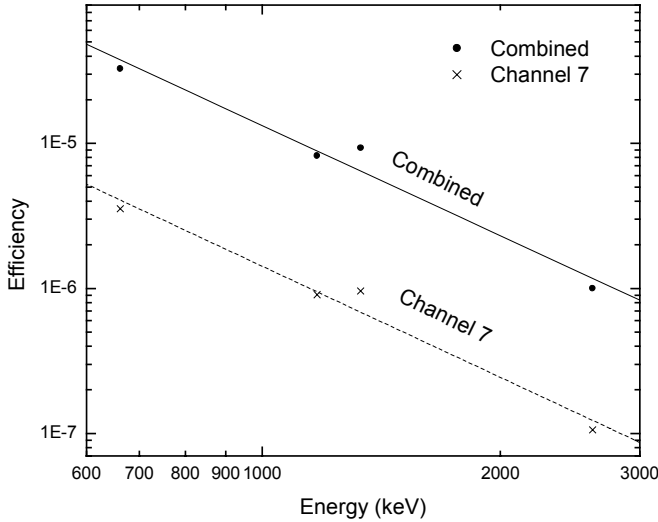


Figure 10. Absolute efficiency for the array of eight $10 \times 10 \times 5 \text{ mm}^3$ detector elements at 19.8 cm.

The efficiency for channel seven is approximately one eighth of the efficiency for the all eight detector elements, as expected. The double escape efficiency is larger than the full-energy efficiency at high energies (Figure 8c and 8d).

4. COMPARISON WITH CALCULATIONS

Some Monte Carlo calculations for the eight-element array were reported in an earlier report.⁵ At 662 keV the absolute efficiency of the array at 19.8 cm is calculated to be 7.29×10^{-5} . The absolute efficiency measured in the present report is $3.80 \times 10^{-5} \pm 5\%$, which is 52% of the calculated value. The calculated absolute efficiency for one detector element, channel 7, is 6.42×10^{-6} . The measured value in the present report is $4.11 \times 10^{-6} \pm 5\%$, which is 64% of the calculated value. The earlier report suggested that the cause of these deficits might be related to the design of the electrodes, the method used to form the spectroscopy signal, and the selection of the material. Additional calculations are in progress, and further investigations of these deficits are planned.

5. CONCLUSIONS

Our results for an array of eight $10 \times 10 \times 5 \text{ mm}^3$ detector elements and an array of four $15 \times 15 \times 7.5 \text{ mm}^3$ detector elements indicate that our approach to achieving good efficiency by combining the signals from a three-dimensional array of large detector elements will work. Simple summing of the signals may be adequate below 2 MeV. However, above 2 MeV, depending on the spectrum, requiring coincidence might be preferred to suppress the Compton continuum and the escapes peaks. In the present work we have extended the earlier results⁵ for the eight element array to higher energies and the earlier results⁴ for the $15 \times 15 \times 7.5 \text{ mm}^3$ detector elements from two to four elements. Twenty-seven large detector elements to build a $3 \times 3 \times 3$ array that we proposed⁴ for measuring high-energy gamma rays ($\leq 10 \text{ MeV}$) were not available because of the low yield in manufacture and the cost. However, our Monte Carlo calculations continue to predict satisfactory performance for such an array for planetary missions. The list-mode data acquisition system we used can be replaced by a simpler system requiring less power.

ACKNOWLEDGMENTS

This work was supported by NASA's Planetary Instrument Definition and Development Program and done under the auspices of the US DOE.

REFERENCES

1. C.E. Moss, K.D. Ianakiev, T.H. Prettyman, R.C. Reedy, M.K. Smith, M.R. Sweet, and J.D. Valentine, "Performance of multi-element CdZnTe detectors," *SPIE* **3768**, pp. 320-329, 1999.
2. T.M. Harrington, J.H. Marshall, J.R. Arnold, L.E. Peterson, J.I. Trombka, and A.E. Metzger, "The Apollo gamma-ray spectrometer," *Nucl. Instr. and Meth.* **118**, pp. 401-411, 1974.
3. W.C. Feldman, B.L. Barraclough, K.R. Fuller, D.J. Lawrence, S. Maurice, M.C. Miller, T.H. Prettyman, and A.B. Binder, "The Lunar Prospector gamma-ray and neutron spectrometers," *Nucl. Instr. and Meth. A* **422**, pp. 562-566, 1999.
4. C.E. Moss, K.D. Ianakiev, T.H. Prettyman, M.K. Smith, and M.R. Sweet, "Multi-element, large-volume CdZnTe detectors," *Nucl. Instr. and Meth. A* **458**, pp. 455-460, 2001.
5. T.H. Prettyman, M.C. Browne, K.D. Ianakiev, C. E. Moss, and S.A. Soldner, "Characterization of a large-volume, multi-element CdZnTe detector," *SPIE* **4141**, pp. 1-10, 2000.
6. The SNO Collaboration, "The Sudbury Neutrino Observatory," *Nucl. Instr. And Meth. A* **411** pp.107-113, 1998.